JOURNAL OF MATERIALS SCIENCE 37 (2002) 51–57

Tensile properties of a few Mg-Li-Zn alloy thin sheets

H. TAKUDA, H. MATSUSAKA
Department of Energy Science and Technology, Kyoto University, Kyoto 606-8501, Japan
E-mail: takuda@energy.kyoto-u.ac.jp

S. KIKUCHI
Department of Materials Science, The University of Shiga Prefecture, Hikone 522-8533, Japan

K. KUBOTA
R&D Center, Mitsui Mining & Smelting Co. Ltd., Ageo 362-0021, Japan

The tensile properties of experimentally produced Mg-6Li-1Zn, Mg-9.5Li-1Zn and Mg-12Li-1Zn alloy thin sheets at room temperature are investigated in this study. Uniaxial tension tests are carried out for various strain rates between 1.4×10^{-5} and 8.3×10^{-2} s^{-1}, and the microstructural and textural changes during the tests are examined. The Mg-6Li-1Zn sheet is composed mainly of the α (hcp) phase and inferior to the other sheets in ductility. The β (bcc) phase is dominant in the Mg-9.5Li-1Zn and Mg-12Li-1Zn sheets, and they have a considerable sensitivity to strain rate. It is observed that the grains are elongated with textural change mainly in the β phase at low strain rates, and the Mg-9.5Li-1Zn and Mg-12Li-1Zn sheets have sufficiently high ductility at low strain rates. The Mg-9.5Li-1Zn sheet composed of $(\alpha + \beta)$ two phase is superior to the Mg-12Li-1Zn sheet of β single phase in the tensile strength.

1. Introduction

Magnesium is one of the lightest and recyclable materials and has high rigidity. Therefore, the use of magnesium in electric appliances and automobiles is drawing much attention from the environmental viewpoint. The forming products of magnesium have been limited, because magnesium is a hexagonal close-packed metal and has poor formability. However, it is well known that the addition of lithium to magnesium gives rise to highly workable, body-centred cubic alloys [1–3]. Lithium is lighter than magnesium. Due to their ultra-low density magnesium-lithium (Mg-Li) alloys are attractive, and investigations on alloy design and metallographical as well as mechanical properties of Mg-Li alloys have long been carried out [1–16].

Mg-Li alloys exhibit two phase structures between 5 and 11 mass% Li contents consisting of the α (hcp) Mg-rich and β (bcc) Li-rich phases at room temperature. The β single phase structure exists for greater than 11 mass% Li contents. The effect of the addition of a third metal on the mechanical properties has also been examined for various third metals by many researchers [2–5, 7, 8, 12–14]. Further, the exhibition of superplastic behaviour has been found in a Mg-9Li alloy by Metenier *et al*. [11] and in a Mg-8Li-1Zn alloy by Kojima *et al*. [12]. However, few studies have examined the formability of Mg-Li alloy thin sheets from a practical point of view.

The authors have recently examined the tensile properties and the press formability of a thin sheet of a Mg-8.5Li-1Zn alloy and found that the sheet has sufficiently high formability at room temperature [17, 18]. In the present study, further, the formability of a few experimentally produced Mg-Li-Zn alloy sheets with various Li contents is examined by uniaxial tension tests under various strain rates. The difference in the tensile properties depending on the Li contents is investigated by means of metallographic observations.

2. Experimental procedure

The materials used in this study are Mg-6mass%Li-1mass%Zn, Mg-9.5mass%Li-1mass%Zn and Mg-12mass%Li-1mass%Zn alloys. The alloys were cast in a high-vacuum induction furnace under an argon atmosphere, annealed at 523 K for 1.8 ks and then warm rolled at 523 K to a thickness of 0.6 mm. The total reduction ratio was about 85%. The Mg-6Li-1Zn, Mg-9.5Li-1Zn and Mg-12Li-1Zn alloy sheets are expressed as materials A, B and C, respectively, in the later description.

Uniaxial tension tests were carried out in the rolling direction. The gauge length and width of the tensile specimens were 50 and 12.5 mm, respectively. The specimens were deformed by a constant cross-head velocity of between 0.05 and 300 mm min^{-1}. The initial strain rates of the tension tests range between 1.4×10^{-5} and 8.3×10^{-2} s^{-1}. The normal anisotropy parameter, r, was measured at the elongation of 15%.

The microstructure and the texture of the specimens before and after the tension tests were examined. The

specimens for optical microscopy were prepared by etching with a nitric acid solution. To contrast the α and the β phases, an acetic acid solution was used. X-ray diffraction analyses were performed using a Philips diffractometer and an automatic texture goniometer with Cu K_α radiation.

3. Results and discussion

Figs 1 and 2 show the X-ray diffraction patterns and the microstructures of the sheets before the tension tests, respectively.

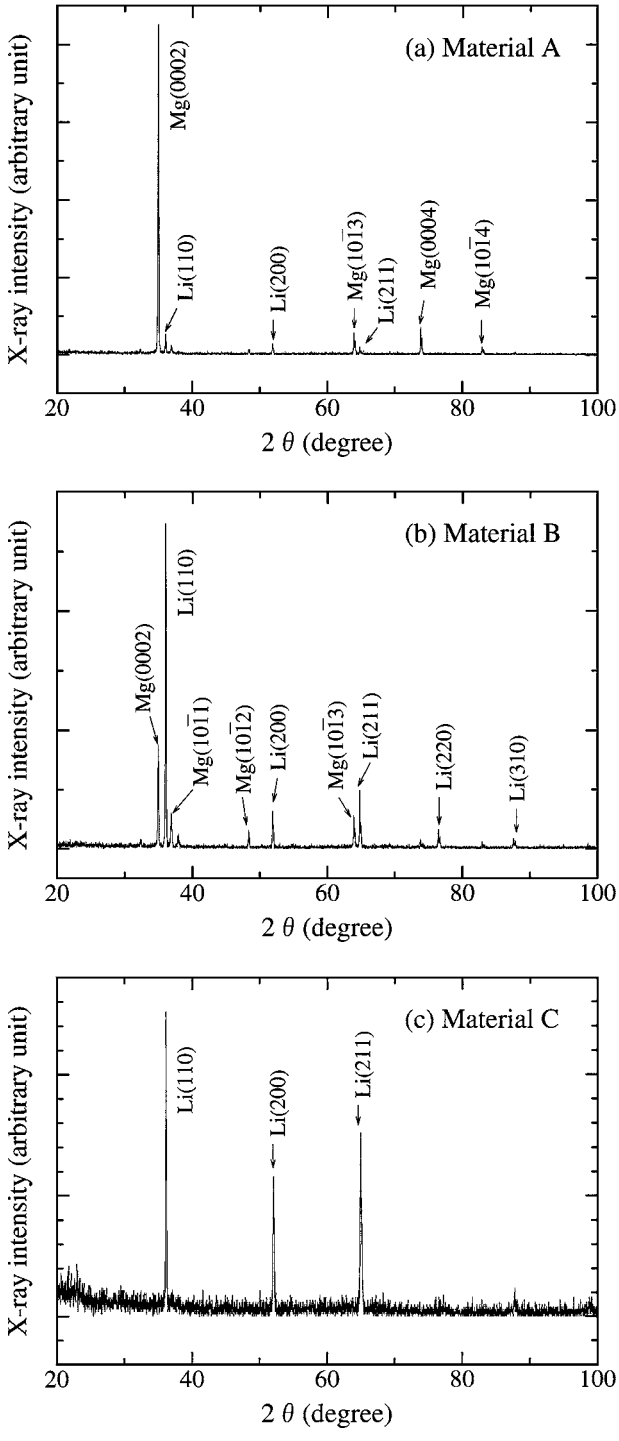

Figure 1 X-ray diffraction patterns of the materials A (Mg-6Li-1Zn), B (Mg-9.5Li-1Zn) and C (Mg-12Li-1Zn) before tension test.

The X-ray diffraction pattern of the material A (Fig. 1a) shows a strong peak of Mg hcp α (0002) plane. Some peaks of Li bcc β planes are also observed though the peak values are relatively low. Therefore, Fig. 1a shows the existence of the β phase in the material A composed mainly of the α phase. Partially recrystallized grains shown in Fig. 2a correspond to the Li-rich β phase. The volume fraction of each phase in the material A is measured to be about 70% α and 30% β.

In the X-ray diffraction patterns of the material B (Fig. 1b), a strong peak of Li bcc (110) plane and other peaks of Li and Mg planes are observed. The material B is also composed of $(\alpha + \beta)$ two phases. The bright and dark zones of the microstructure shown in Fig. 2b correspond to the α and β phases, respectively. The volume fraction of each phase is about 30% α and 70% β for the material B. The grains are elongated in the rolling direction.

Fig. 1c shows the peaks only of Li bcc planes and that the material C consists of the β single phase. In contrast with the microstructure of the material B, equiaxial and large grains are observed in the microstructure of the material C (Fig. 2c). The mean grain diameter is about 100 μm.

Fig. 3 shows the true stress-strain $(\sigma - \varepsilon)$ curves of the materials A, B and C obtained from uniaxial tension tests under the condition that the initial strain rate is $8.3 \times 10^{-4}\ s^{-1}$. The tensile properties in this case are indicated in Table I. The tensile strength of the material A is higher than those of the materials B and C, though the proof stresses of the three materials are almost equal. The work-hardening exponent, n (in the approximation of $\sigma = F\varepsilon^n$), for the material A is larger than those for the materials B and C. However, the materials B and C are superior to the material A in the elongation. It is notable that the material B is superior to the material C not only in the tensile strength but also in the elongation. The normal anisotropy parameter, r, of the material A is very high, as is usual with hcp metals. On the other hand, the r-values of the materials B and C are somewhat smaller than 1.0 because the hcp phase is not dominant for these materials.

Fig. 4 shows the true stress-strain relationships for various initial strain rates. The elongation increases with decrease in the strain rate for all the materials. In comparison with the material A, however, the materials B and C are very sensitive to strain rate. At the comparatively low strain rates the elongation reaches about 100% for the materials B and C. As mentioned above, the tensile specimens are not small, but have the long gauge length of 50 mm. It is notable that such large elongations are obtained in the long specimens. It may be better that the forming of the sheets is operated at lower strain rates. A remarkable feature of the materials B and C is that not only the elongation, but also the stress value greatly depends upon the strain rate. The stress increases notably with the strain rate. It is very interesting that the materials B and C have the strain rate sensitivity even at room temperature as if at elevated temperatures. This may be due to the low melting point of lithium (454 K).

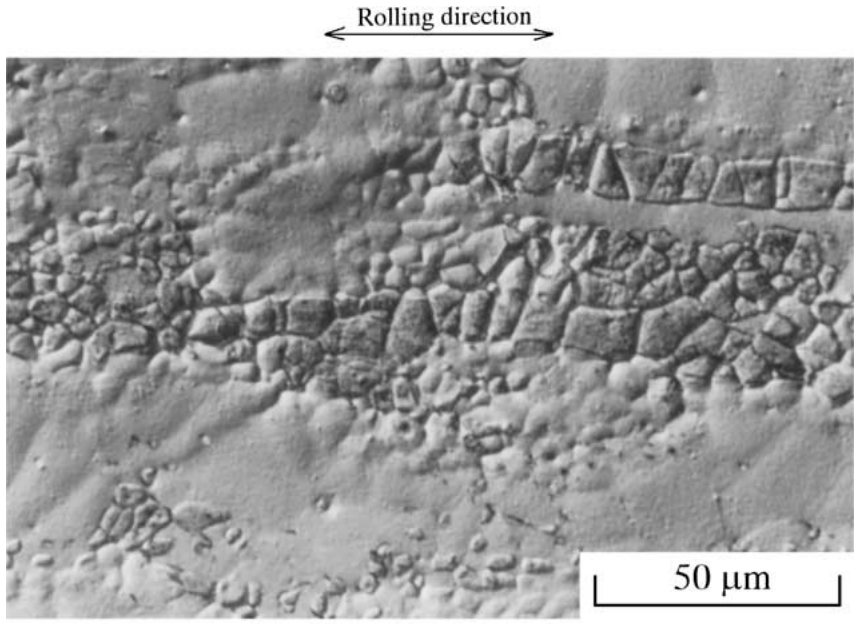

(a) Material A

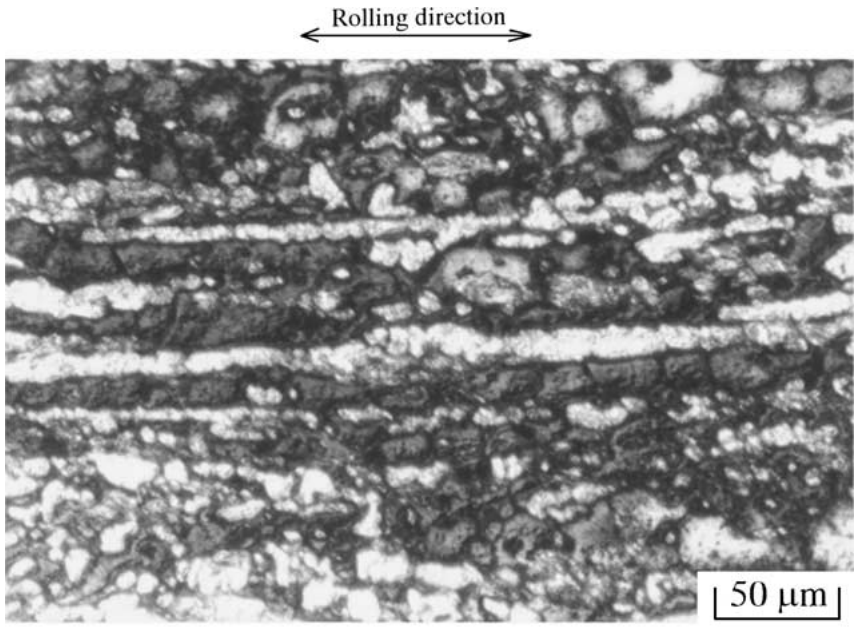

(b) Material B

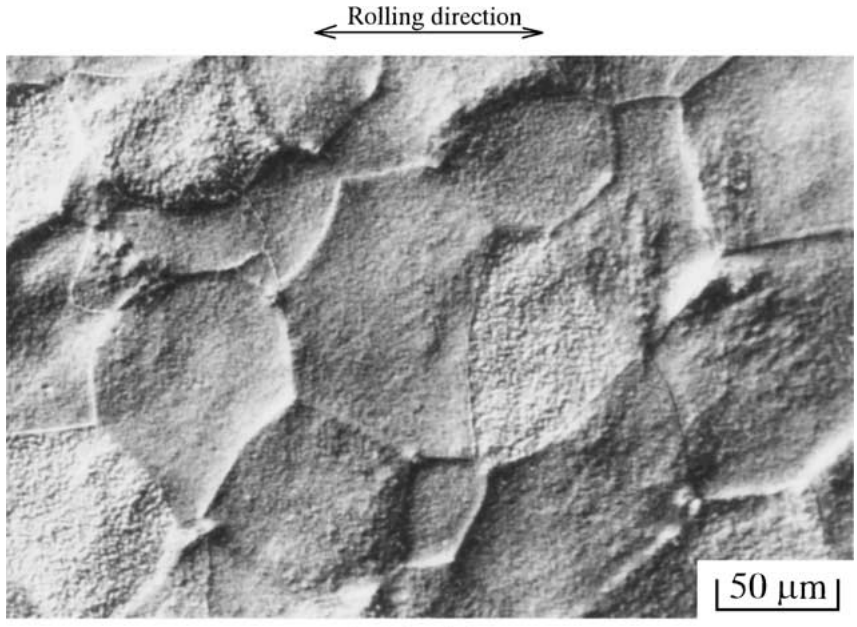

(c) Material C

Figure 2 Microstructures of the materials A, B and C before tension test.

TABLE I Tensile properties of the materials A, B and C obtained from uniaxial tension tests for an initial stain rate of 8.3×10^{-4} s^{-1}

Material	A	B	C
Proof stress (MPa)	112	121	124
Tensile strength (MPa)	155	134	125
Elongation (%)	32.2	71.4	56.0
Work-hardening exponent, n	0.15	0.06	0.00
Normal anisotropy parameter, r	5.98	0.87	0.70

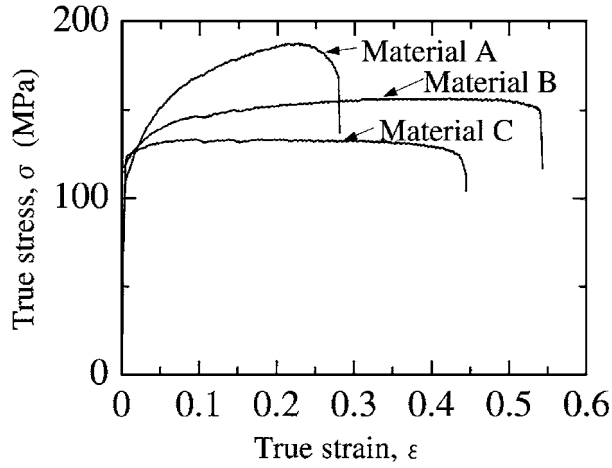

Figure 3 True stress-strain relationships of the materials A, B and C for an initial strain rate of 8.3×10^{-4} s^{-1}.

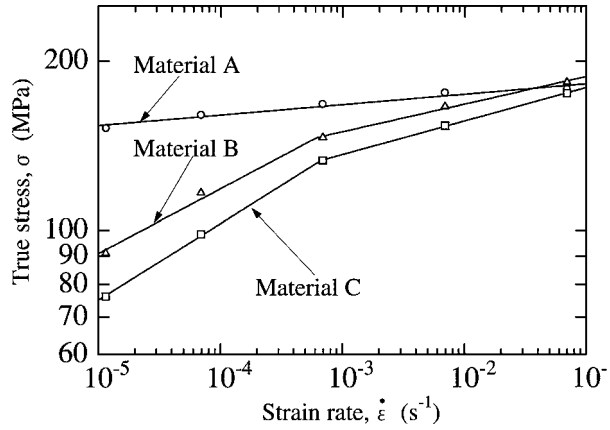

Figure 5 Relationships between true stress and strain rate in log-log scale for a strain of 0.1.

Fig. 5 shows the relationships between the stress, σ, and the strain rate, $\dot{\varepsilon}$, in log - log scale. The linear relationship exists between the logarithms of σ and $\dot{\varepsilon}$. Namely, $\sigma = K\dot{\varepsilon}^m$ stands. The strain-rate sensitivity exponent, m, for the material A is small and evaluated to be a constant value of 0.02. The m-values for the materials B and C are 0.12 and 0.14 at lower strain rates, and are 0.05 and 0.06 at higher strain rates, respectively. There may be a relation between the high m-value and the high ductility at lower strain rates for the materials B and C.

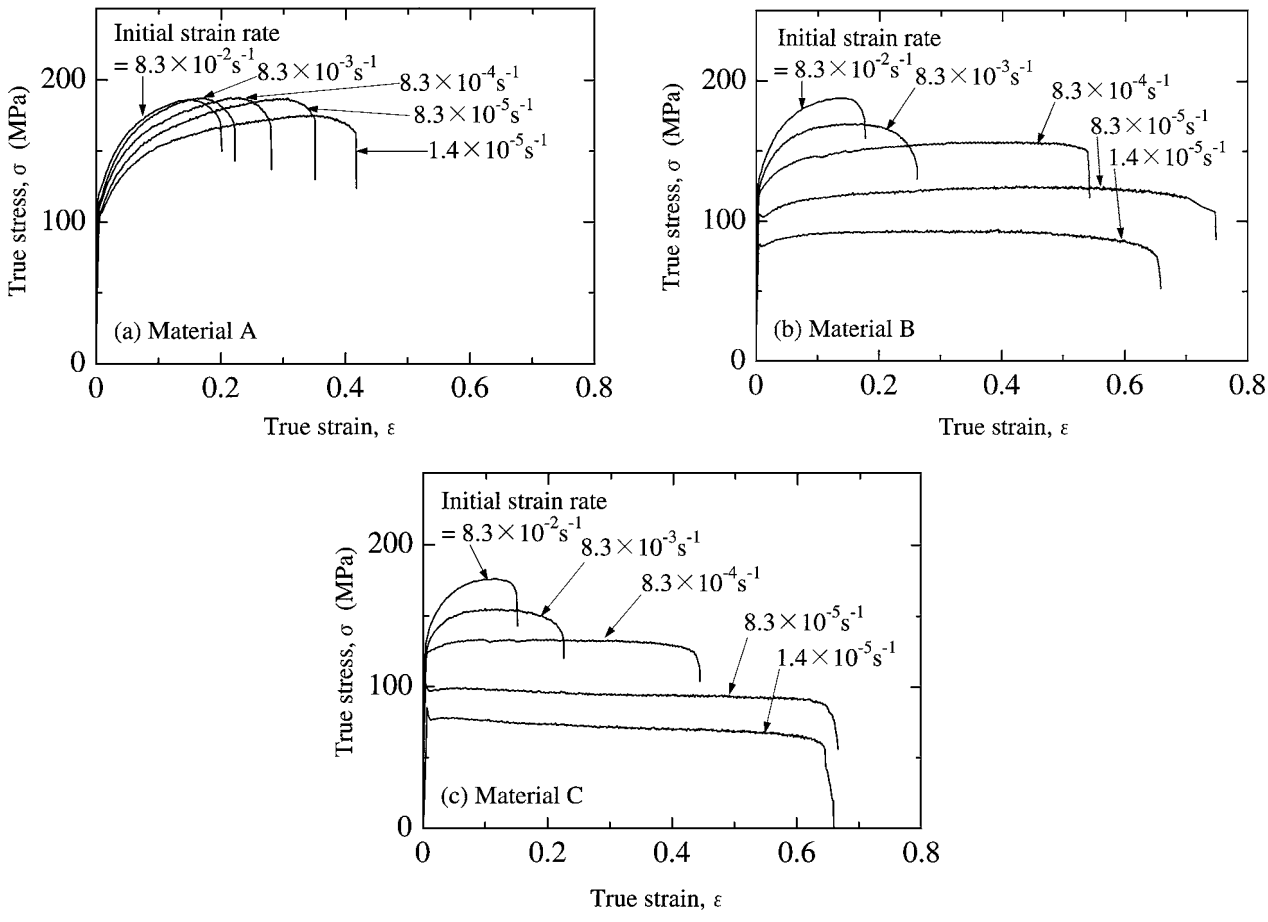

Figure 4 True stress-strain relationships of the materials A, B and C for various strain rates.

Fig. 6 shows the X-ray diffraction patterns of the sheets after the tension tests under the condition that the initial strain rate is low at 1.4×10^{-5} s^{-1}. The change in the texture during the tension tests can be seen by comparing Fig. 6 with Fig. 1. For the material A composed mainly of the α phase, there is no obvious change in the texture and the microstructure during the tension tests. On the other hand, for the materials B and C the change in the X-ray intensity of the Li bcc β planes is observed. While the (110) plane is mainly orientated before the tension tests (Fig. 1b and c), the peaks of the (200) and (211) planes become higher than the (110) plane during the tension tests. As is exemplified by the pole figure of Fig. 7, the texture of the β phase of the materials B and C turns to be composed mainly of (001)[$\bar{1}$10] and (112)[$\bar{1}$10].

Fig. 8 shows the microstructures of the materials B (Fig. 8a) and C (Fig. 8b) after the tension tests for the low strain rate of 1.4×10^{-5} s^{-1}. The grains are elongated to the tensile direction during the tension tests.

The results similar to the above ones shown in Figs 6–8 are observed for the strain rates lower than 8.3×10^{-4} s^{-1}. For the strain rates higher than 8.3×10^{-3} s^{-1}, the textural and the microstructural changes are small and not clear because of the small elongation during the tension tests. The low strain rate enables the textural change in the β phase and the elongation of the grains in the tensile direction for the materials B and C.

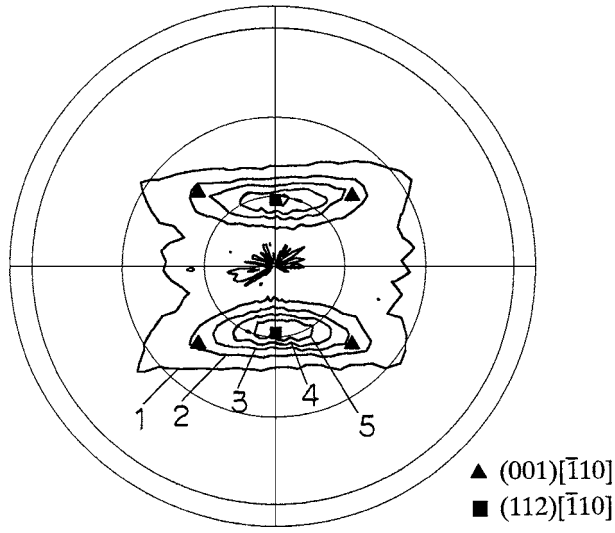

Figure 7 (110) pole figure of β phase of the material C after tension test for an initial strain rate of 1.4×10^{-5} s^{-1}.

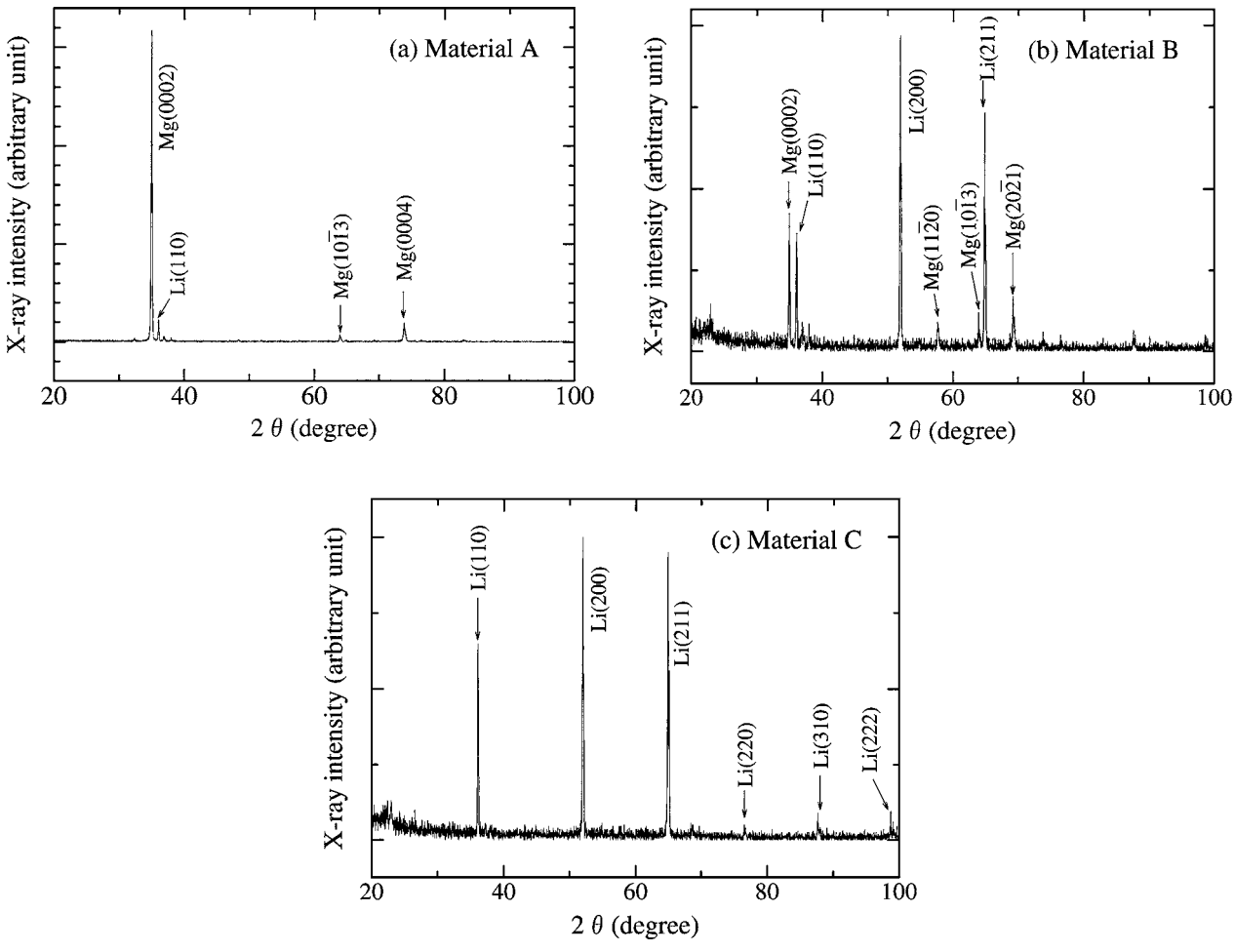

Figure 6 X-ray diffraction patterns of the materials A, B and C after tension test for an initial strain rate of 1.4×10^{-5} s^{-1}.

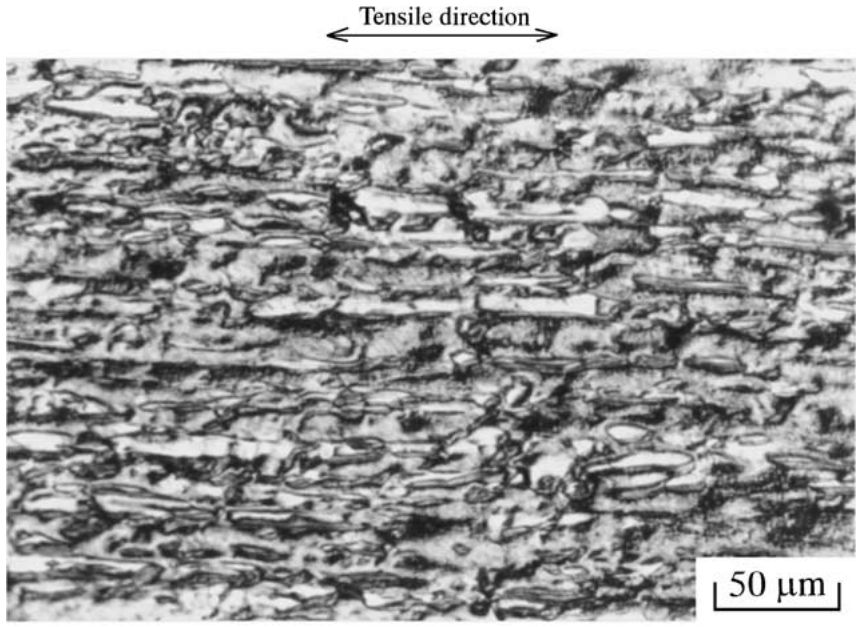

(a) Material B

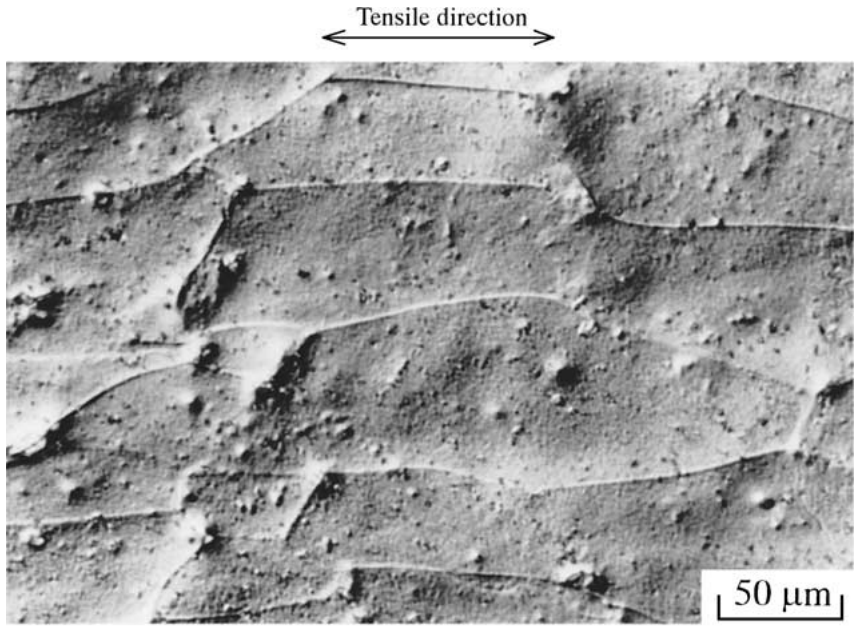

(b) Material C

Figure 8 Microstructures of the materials B and C after tension test for an initial strain rate of 1.4×10^{-5} s^{-1}.

4. Conclusions

In this study, the formability of a few experimentally produced Mg-Li-Zn alloy thin sheets was investigated. Uniaxial tension tests were carried out at room temperature for various strain rates between 1.4×10^{-5} and 8.3×10^{-2} s^{-1}. The metallographic changes during the tests were observed and the results are summarised as follows:

1. In the Mg-6Li-1Zn alloy sheet the α (hcp) phase is dominant, and therefore the ductility of the sheet is not high.
2. The Mg-9.5Li-1Zn and Mg-12Li-1Zn alloy sheets have high ductility at comparatively low strain rates. The maximum elongation reaches 100%.
3. The low strain rate enables the textural change in the β (bcc) phase and the elongation of the grains in the tensile direction for the Mg-9.5Li-1Zn and Mg-12Li-1Zn alloy sheets.
4. Taking the higher rigidity into consideration, it may be concluded that the Mg-9.5Li-1Zn alloy sheet composed of $(\alpha + \beta)$ two phases is superior to the Mg-12Li-1Zn alloy sheet composed of β single phase.

References

1. J. H. JACKSON, P. D. FROST, A. C. LOONAM, L. W. EASTWOOD and C. H. LORIG, *Trans. AIME* **185** (1949) 149.
2. R. S. BUSK, D. L. LEMAN and J. J. CASEY, *ibid.* **188** (1950) 945.
3. P. D. FROST, J. G. KURA and L. W. EASTWOOD, *ibid.* **188** (1950) 1277.
4. W. E. FREETH and G. V. RAYNOR, *J. Inst. Metals* **82** (1953–54) 575.

5. W. R. D. JONES, *ibid.* **84** (1955–56) 364.
6. M. W. TOAZ and E. J. RIPLING, *ibid.* **85** (1956–57) 137.
7. G. V. RAYNOR and J. R. KENCH, *ibid.* **88** (1959–60) 209.
8. J. C. McDONALD, *ibid.* **97** (1969) 353.
9. R. E. LEE and W. J. D. JONES, *J. Mater. Sci.* **9** (1974) 469.
10. M. SAHOO and J. T. N. ATKINSON, *ibid.* **17** (1982) 3564.
11. P. METENIER, G. GONZÁLEZ-DONCEL, O. A. RUANO, J. WOLFENSTINE and O. D. SHERBY, *Mater. Sci. Eng. A* **125** (1990) 195.
12. Y. KOJIMA, M. INOUE and O. TANNO, *J. Jpn. Inst. Metals* **54** (1990) 354.
13. S. HORI and W. FUJITANI, *J. Jpn. Inst. Light Metals* **40** (1990) 285.
14. K. MATSUZAWA, T. KOSHIHARA, S. OCHIAI and Y. KOJIMA, *ibid.* **40** (1990) 659.
15. T. MUKAI, K. ISHIKAWA, Y. OKANDA, M. MABUCHI, K. KUBOTA and K. HIGASHI, in Proceedings of the Third Light Weight Alloys for Aerospace Applications symposium, Las Vegas, February 1995, edited by E. W. Lee, N. J. Kim, K. V. Jata and W. E. Frazier (The Minerals, Metals & Materials Society, 1995) p. 483.
16. N. SAITO, M. MABUCHI, M. NAKANISHI, K. KUBOTA and K. HIGASHI, *Scripta Materialia* **36** (1997) 551.
17. H. TAKUDA, S. KIKUCHI, T. TSUKADA, K. KUBOTA and N. HATTA, *Mater. Sci. Eng. A* **271** (1999) 251.
18. H. TAKUDA, T. ENAMI, K. KUBOTA and N. HATTA, *J. Mater. Process. Technol.* **101** (2000) 281.

Received 21 March
and accepted 28 August 2001